Cretaceous metamorphism of metacarbonates in the Austroalpine Schneeberg complex, Tirol*

by *Georg Hoinkes***

Abstract

In siliceous dolomites of the Schneeberg complex talc and tremolite formed during progressive Early Alpine metamorphism. Substitution of FeO for MgO, although shifting the equilibrium temperatures only slightly, reduces the stability field of talc and calcite in the T-X_{CO_2}-plane significantly due to acute intersection of equilibrium curves. Equilibrium temperatures of $\sim 560\,°C$ are deduced for the assemblage Dol–Qua–Tal–Tre–Cal by means of Cal–Dol-thermometry. Significant impurities in solids besides FeO are sometimes K_2O, Na_2O and Al_2O_3 and lead to phlogopite and chlorite before tremolite which exhibits a continuous compositional change to pargasitic amphibole. The only occurrence of diopside results from a progressive reaction of pargasitic amphibole and calcite to diopside and garnet. Breakdown of tremolite to talc is thought to be a retrograde alteration during cooling after peak of Early Alpine metamorphism and no hints for a pre-Alpine crystallisation are seen from the metacarbonates in the Schneeberg complex although Hercynian mineral phases may be obscured by the Early Alpine event.

Introduction

The Austroalpine Ötztal unit consists of polymetamorphic proterozoic to early paleozoic basement rocks and a fragmentary metasedimentary cover of paleozoic to mesozoic age. The only occurrence of paleozoic metasediments is restricted to the Schneeberg complex which forms complicated narrow synclines to the south of the Ötztal alps (Fig. 1). At least three distinct synclines can be devided due to their differring lithology and the overall lithology of the Schneeberg complex is differring from the Ötztal basement rocks (SCHMIDEGG, 1933).

Metasediments of the Schneeberg complex are characterized by metacarbonates, metamarls and metapelites in contrast to the quartzofeldspatic basement where metacarbonates are missing.

---

* *Dedicated to Dr. Oskar Schmidegg on occasion of his 85th birthday.*
** Institut für Mineralogie und Petrographie der Universität, Universitätsstrasse 4, A-6020 Innsbruck, Austria.

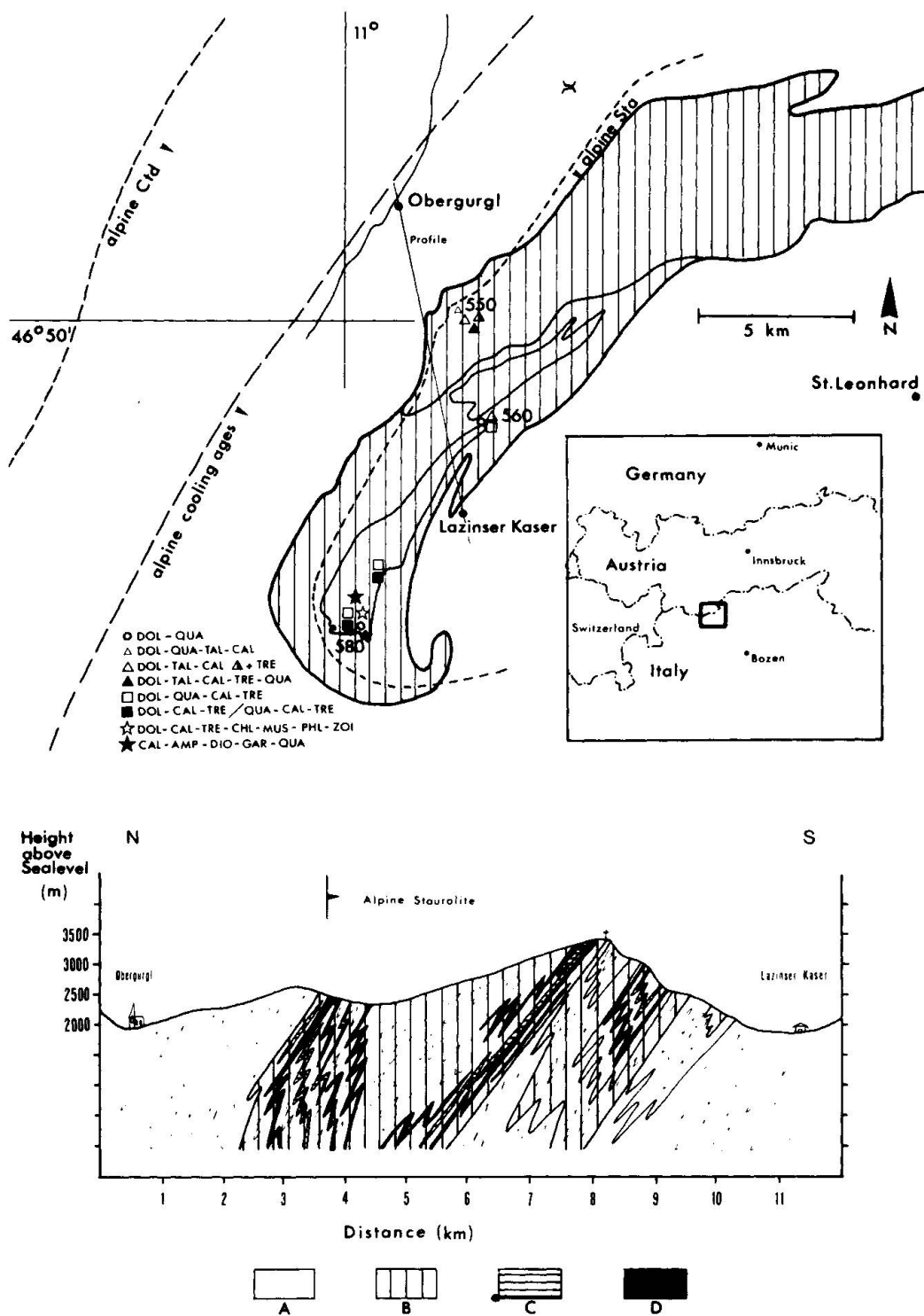*Fig. 1*   a) Outline geological map of the southern Ötztal alps, showing narrow and elongated occurrence of the Schneeberg complex.
   b) Profile as indicated in the map, showing the isoclinally folded synclines.
      Numbers give T°C due to Cal–Dol thermometry.
      A = polymetamorphic basement
      B = Schneeberg complex
      C = Amphibole rocks (including amphibolites and amphibole schists)
      D = Metacarbonates

An intensive Cretaceous metamorphism of the Schneeberg synclines together with their basement is now well established due to K/Ar- and Rb/Sr-cooling ages of micas which range between 90–75 my (SCHMIDT et al., 1967, SATIR, 1975, THÖNI, 1981).

In the basement an uncertain Cambrian/Ordovizian and a proofed Hercynian high grade metamorphism preceded the Cretaceous event in contrast to the Schneeberg rocks, where the grade of the Hercynian overprint is thought to be rather low but is still matter of discussion.

This paper is concerned with the phase petrology of the metacarbonates to derive metamorphic conditions of the Cretaceous event and to look for indications for an Hercynian overprint.

Mineral assemblages and mineral reactions

Metacarbonates of the Schneeberg synclines, occurring as both, small lenses and massive layers show variations in colour from pure white, yellowish to dark grey which certainly is a function of chemistry. Pure white marbles only refer to the siliceous carbonate system $CaO-MgO-SiO_2-H_2O-CO_2$. Additional Al_2O_3, K_2O and FeO are the most important impurities.

The following assemblages of petrogenetic significance have been observed in metacarbonates referring to the siliceous carbonate system:

(a) dolomite + quartz
(b) dolomite + quartz + talc + calcite
(c) dolomite + quartz + talc + calcite + tremolite (Fig. 2)
(d) dolomite + talc + calcite + tremolite
(e) dolomite + quartz + calcite + tremolite
(f) dolomite + calcite + tremolite
(g) quartz + calcite + tremolite

In order to achieve these uni-, di- and multivariant assemblages the following reactions may have been passed during progressive metamorphism.

(1) $3\,Dol + 4\,Qua + 1\,H_2O = 1\,Tal + 3\,Cal + 3\,CO_2$
(2) $5\,Tal + 6\,Cal + 4\,Qua = 3\,Tre + 6\,CO_2 + 2\,H_2O$
(3) $2\,Tal + 3\,Cal = 1\,Tre + 1\,Dol + 1\,CO_2 + 1\,H_2O$
(4) $5\,Dol + 8\,Qua + 1\,H_2O = 1\,Tre + 3\,Cal + 7\,CO_2$

In impure dolomitic metacarbonates the assemblage:

(h) dolomite + calcite + tremolite + chlorite + muscovite + phlogopite + zoisite

is observed but no progressive reaction sequence can be deduced from the field
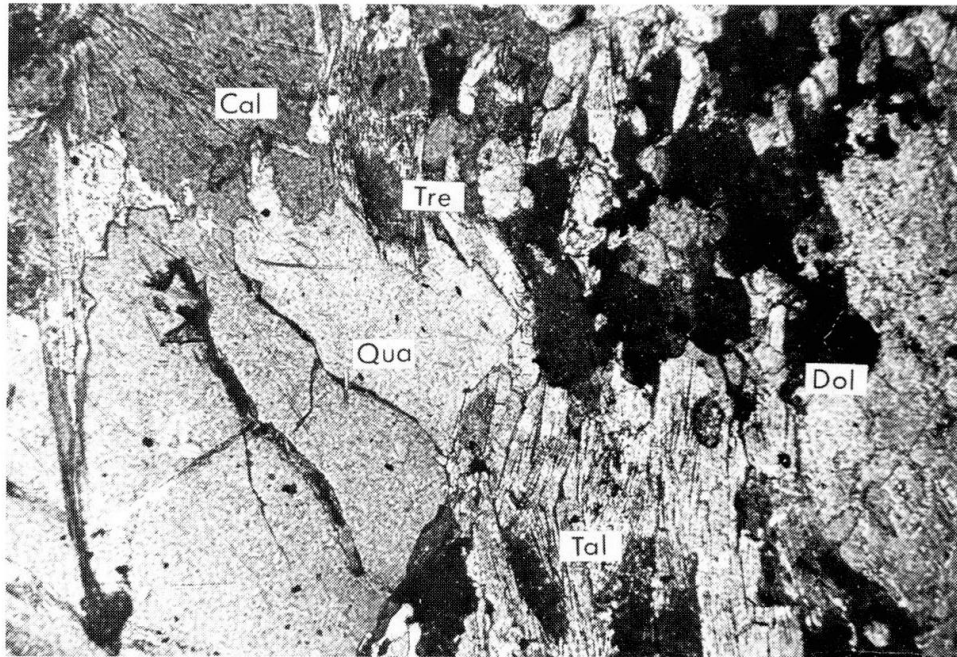
Fig. 2   Photomicrograph of the five-phase assemblage dol + cal + tre + tal + qua in sample Gl 135.
Crossed polarised light. Shown area: 1.4 x 2 mm.
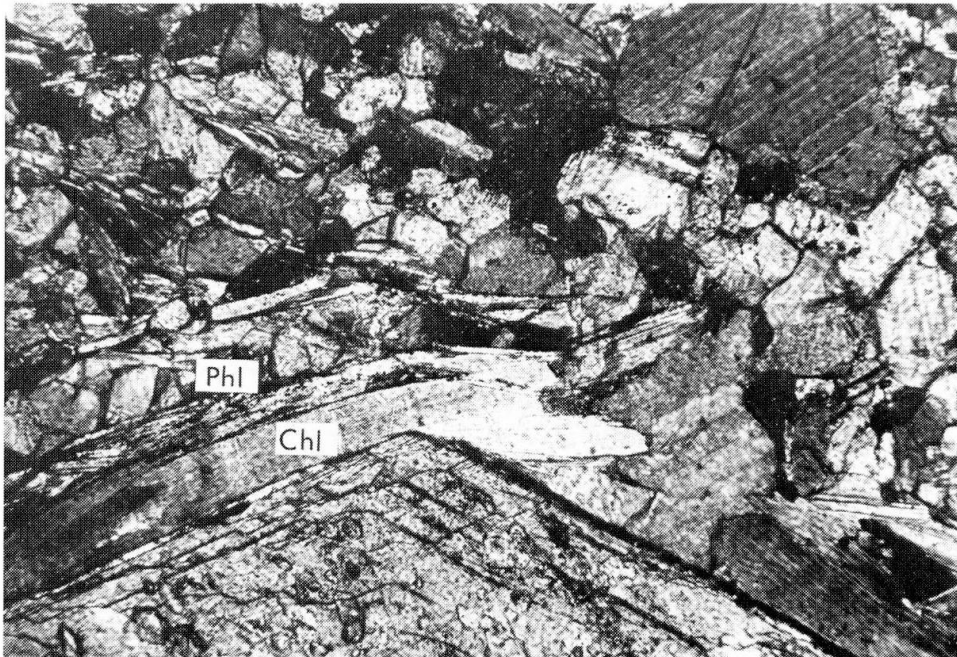
Fig. 3   Photomicrograph of tremolite, chlorite and phlogopite in carbonate matrix (S 9).
Note that chlorite is affected by growing tremolite.
Crossed polarised light. Shown area: 1.4 x 2 mm.
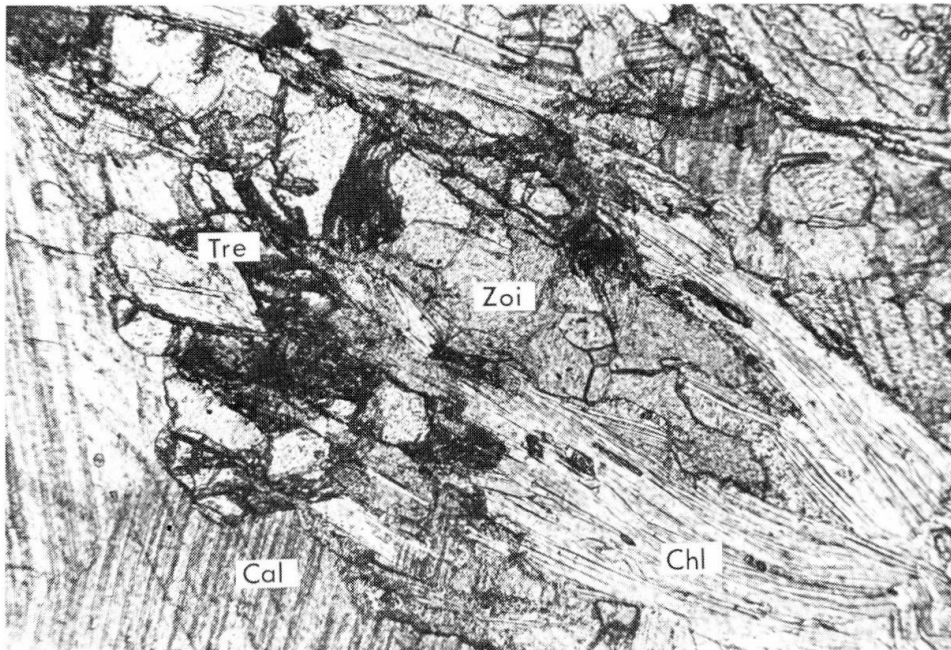
Fig. 4 Photomicrograph of textures indicating reaction (6): Chlorite + calcite + quartz = tremolite + zoisite.
Plane polarised light. Shown area: 1.4 x 2 mm.
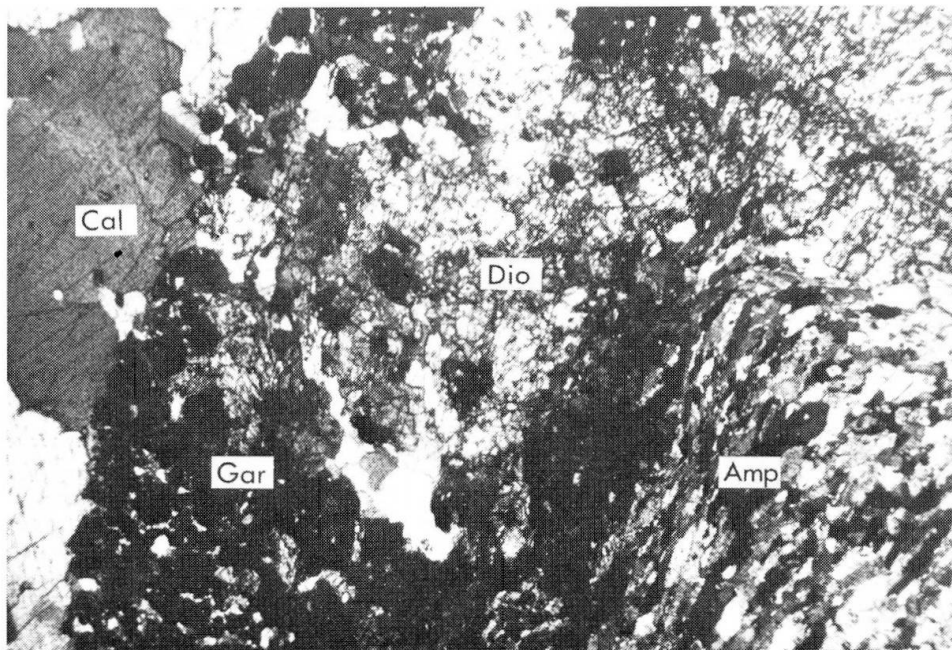
Fig. 5 Photomicrograph of diopside- and garnet- intergrowth forming a reaction layer between calcite (left) and
amphibole (right). Crossed polarised light.
Shown area: 9 x 13 mm.

due to rare occurrence of rocks referring to this chemical system containing additional K_2O and Al_2O_3. Quartz is absent in this assemblage. Pushing aside textures between tremolite and chlorite (Fig. 3) indicate that chlorite was prior to tremolite. Intergrowth textures of chlorite with phlogopite (Fig. 3) as well as tremolite with zoisite (Fig. 4) speak in favour of simultaneous crystallization of these mineral pairs. Therefrom the following reaction sequence with rising temperature may be inferred:

(5) Mus + Dol + Qua + H_2O = Bio + Chl + Cal + CO_2
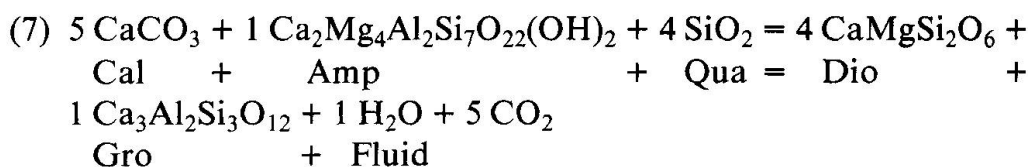(6) Chl + Cal + Qua = Tre + Zoi + H_2O + CO_2
(4) Dol + Qua + H_2O = Tre + Cal + CO_2

Another mineral assemblage of impure metacarbonates occurs as a reaction zone between calcite marble and amphibolite (Fig. 5):

(i) calcite + calcic amphibole + diopside + garnet + quartz

which is obviously due to the schematic reaction:

(7) $5 CaCO_3$ + $1 Ca_2Mg_4Al_2Si_7O_{22}(OH)_2$ + $4 SiO_2$ = $4 CaMgSi_2O_6$ +
     Cal   +   Amp   +   Qua =   Dio   +
     $1 Ca_3Al_2Si_3O_{12}$ + $1 H_2O$ + $5 CO_2$
     Gro   + Fluid

The field occurrence of assemblages (a) to (i) is indicated in Fig. 1. At least the distribution of the isochemical assemblages (a) to (g) seems to be a function of metamorphic grade (and fluid). Retrograde alteration of tremolite lead to total or only partly pseudomorphs of talc and calcite (HOINKES & PURTSCHELLER, 1976). Textures therefore clearly indicate two generations of talc and calcite, whereas all other phases do not allow a distinction between two possible generations.

Chemistry of mineral phases

CARBONATES

Chemistry of calcites coexisting with dolomite, either alone or as part of isobarically in- and univariant assemblages are shown in table 1. $MgCO_3$-solid solution in calcites coexisting with dolomite is a very capable and often applied geothermometer in the temperature range of amphibolite facies (for example: PUHAN, 1976, BICKLE & POWELL, 1977, RICE, 1977, JANSEN et al., 1978, NESBITT & ESSENE, 1982). The geothermometer is based on the solvus in the system $CaCO_3$–

Tab. 1   Composition of some calcites coexisting with dolomite.

wt%	GL 135 (n = 41) m	s	S 12b (n = 47) m	s	S 13 (n = 36) m	s	2/1$^{x)}$ (n = 56)		3/2$^{x)}$ (n = 61)		retrograde (n = 20)	
CaO	53.27	3.14	52.50	2.94	53.33	1.22	52.75	1.30	53.13	0.89	55.62	1.94
MgO	1.88	0.27	2.45	0.26	2.27	0.37	2.65	0.99	2.39	0.64	0.45	0.20
FeO	1.38	0.21	0.28	0.07	0.07	0.03	0.22	0.06	0.03	0.01	0.02	0.02
MnO	0.26	0.09	-	-	0.03	0.01	0.01	-	0.01	-	-	
CO$_2$$^{c)}$	44.84		44.05		44.39		44.43		44.33		44.15	
total	101.63		99.82		100.09		100.06		99.89		100.24	
Mol%												
CaCO$_3$	93.18		93.54		94.28		93.17		94.05		98.85	
MgCO$_3$	4.57		6.07		5.58		6.51		5.89		1.12	
FeCO$_3$	1.88		0.39		0.10		0.31		0.04		0.03	
MnCO$_3$	0.36		-		0.04		0.01		0.01		-	
MgCO$_3$^{t}	5.58		6.35		5.64		6.74		5.92		1.12	
T°C^{r}	552		575		554		586		563		342	

x   =   exsolved
t   =   corrected for FeCO$_3$ according to TALANTSEV (1978)
r   =   according to RICE (1977)
c   =   calculated stoichiometrically
m   =   mean value
s   =   standard deviation

CaMg(CO$_3$)$_2$ which was originally studied by HARKER & TUTTLE (1955) and GRAF & GOLDSMITH (1955). RICE (1977) derived a solvus equation by means of least squares analysis of experimental data of GRAF & GOLDSMITH (1955) and GOLDSMITH & NEWTON (1969) which was used to determine equilibrium temperatures given in tab. 1 and fig. 6.

$$(I) \qquad \log X^{Cal}_{MgCO_3} \quad = \quad \frac{-1690}{T(K)} \quad + \quad 0.795$$

The chemistry of calcites deviate from Ca–Mg solid solution due to Fe and Mn (Tab. 1). FeCO$_3$ content of calcites not taken into account results in temperatures too low by about 25°C per mol % FeCO$_3$. In these cases the value of $X^{Cal}_{MgCO_3}$ were corrected using the procedure given by TALANTSEV (1978) who fitted experimental data for the Fe-bearing carbonate system from ROSENBERG (1967) and GOLDSMITH et al. (1962):

$$(II) \qquad X^{Cal}_{MgCO_3} = X^{Cal}_{MgCO_3} \cdot (1+11.5 \ X^{Cal}_{FeCO_3} + 5 X^2_{FeCO_3} + 550 \ X^3_{FeCO_3})$$

Chemistry of carbonates were measured by a TV-scanned electron beam of the size of about 20 μm². Before measurement the calcites were checked for dolomite exsolution by means of BSE-scanning, which is a common phenomenon due to cooling after peak of metamorphism. If exsolution was observed it was attempted to obtain average composition of the whole calcite grain. This meth-
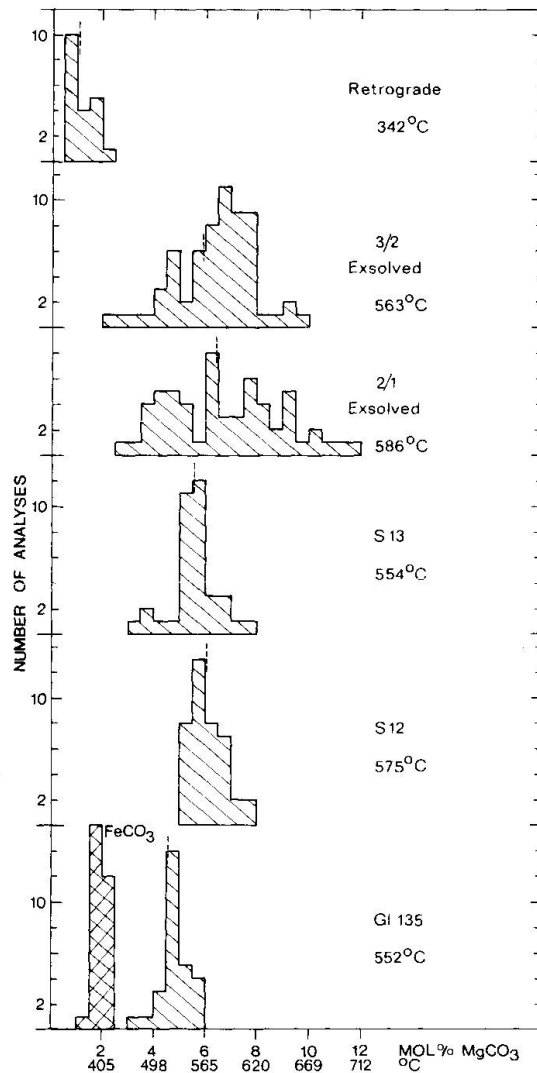
Fig. 6   Histograms of the $MgCO_3$-(and $FeCO_3$)-content of calcites coexisting with dolomite.
Gl 135, S 12 and S 13 represent single samples, 2/1 and 3/2 represent single grains and retrograde calcites represent various samples.

od resulted in a large scatter of X_{MgCO_3}-values but temperatures derived from the mean values of single exsolved calcite grains were equivalent to temperatures derived from homogeneous calcite grains (Fig. 6).

Equilibrium temperatures for prograde calcite–dolomite pairs vary between 550 and 580 °C and fit well with results from the garnet–biotite-exchange thermometer in accompanying metapelites (HOINKES, 1981). It can be seen from fig. 6 and tab. 1 that retrograde calcites have remarkable low $MgCO_3$-contents when compared with prograde calcites. If breakdown of tremolite is due to retrograde occurrence of reaction (3), as inferred from textures shown in HOINKES & PURTSCHELLER (1976, Fig. 2) where dolomite and calcite are involved, low X_{MgCO_3}-values in retrograde calcites reflect low equilibrium temperatures in the

range of about 300 °C. (This value gives an order of magnitude only since the solvus tends to get very steep with decreasing temperatures.) On the other hand textures sometimes also indicate retrograde occurrence of reaction (2) where $X_{MgCO_3}^{Cal}$-values in calcites are in the same low range but are not temperature-significant.

SILICATES

Fluor in silicate phases

Additional fluor may be present in metacarbonates in significant amounts and then effects stability fields of phases seriously (SKIPPEN, 1974, MOORE & KERRICK, 1976, JANSEN et al., 1978, KEARNS et al., 1980, MERCOLLI, 1980, HOSCHEK, 1980, METZ, 1981). It is therefore important to point out, that mineral phases of metacarbonates in the Schneeberg complex have very low F-contents only (Tab. 2). The highest recorded values in the silicate phases are: phlogopite: 0.8%, tremolite: 0.4%, talc: 0.3% and chlorite: 0.2%. The effect of F on the reaction-curve topology in the pure siliceous carbonate system is therefore neglected in the present study.

Amphibole

Chemistry of amphiboles deviate from pure tremolite to pargasitic composition mainly due to coupled substitution of tschermak vector $(Mg_{-1}Si_{-1}Al_2)$ and edenite vector $(\square_{-1}^A Si_{-1}^{IV} Na^A Al^{IV})$ (Fig. 7 a). There is no good correlation between Na in the M(4) site and Al^{IV} which means that glaucophane substitution $(Ca_{-1}^{M4} Mg_{-1}^{VI} Na^{M4} Al^{VI})$ was not very pronounced (Fig. 7 b). Besides these coupled substitutions the simple $FeMg_{-1}$ exchange vector was effective to variable extents (Tab. 2). Since Fe^{+3}/Fe^{+2} cannot be determined with electron microprobe methods the question of Fe^{+3} content and possible exchange vectors involving Fe^{+3} in amphiboles is not considered here. The continuous change in composition shown in Fig. 7 a, where a miscibility gap is missing although postulated by many authors (see GRAPES and GRAHAM, 1978 for review) is thought to be due to the occurrence of continuous reactions in terms of tschermak vector among the ACF-phases involved in equilibrium (7) as illustrated in Fig. 8. These reactions may occur during a prograde metamorphic event and hence patches of different compositions within single amphiboles must not be related to different generations of crystallisation.
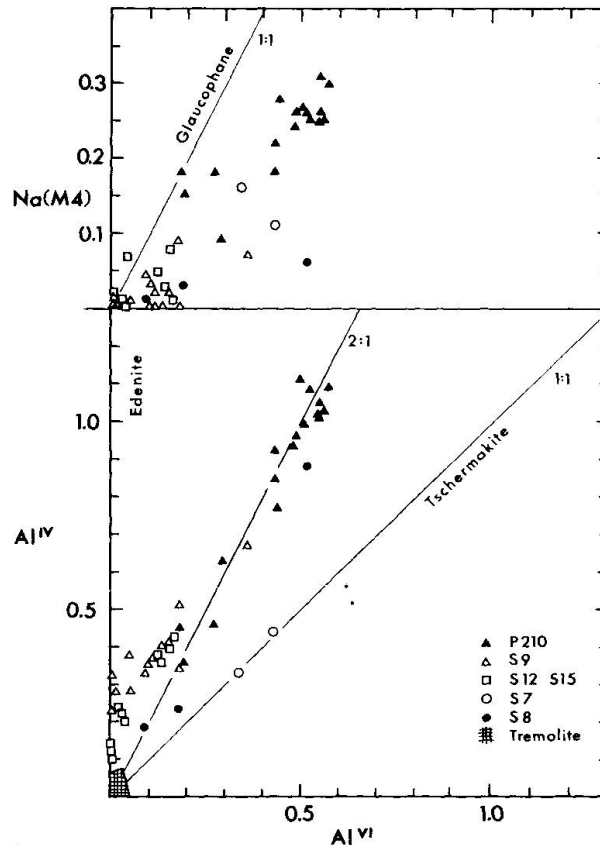
Fig. 7 Plot of Al^{VI} versus Al^{IV} and Al^{VI} versus Na(M4) for amphiboles investigated in this study. Different symbols represent different samples.

Diopside

Absence of diopside in pure marbles limits metamorphic grade at the hight temperature side. However a single occurrence of diopside in impure metacarbonates was observed (Fig. 5). Chemical composition of natural diopside deviates from pure endmember composition only slightly in terms of jadeite substitution Mg$_{-1}$ Ca$_{-1}$ NaAl combined with tschermak substitution (Tab. 2). FeMg$_{-1}$ exchange is significant with more than 30 mol % Fe-endmember but is more pronounced in coexisting amphiboles (Tab. 2).

Garnet

in reaction (7) involved as pure grossular deviates in nature significantly from this idealized composition. Its chemistry is characterised by almandine-grossular solid solution with minor amounts of pyrope and spessartine molecule (Tab. 2). Chemical zoning with decreases of MnO and increases of FeO, MgO and CaO towards the rims is observed.

Tab. 2 Selected microprobe analyses of coexisting silicate phases.

wt%	PL 92 Tre	PL 92 Tal	PL 92 Tal³⁾	GL 135 Tre	GL 135 Tal	S 9 Tre	S 9 Chl	S 9 Phl	S 9 Zoi	P 210 Hbl	P 210 Hbl	P 210 Dio	P 210 Gar (c)	P 210 Gar (r)
SiO₂	58.57	61.30	63.29	56.60	57.20	54.90	29.10	41.80	38.37	50.90	46.00	50.90	37.53	38.32
TiO₂	0.00	0.02	0.00	0.00	0.00	0.05	0.04	0.54	0.00	0.12	0.37	0.06	0.06	0.06
Al₂O₃	0.62	0.31	0.34	0.07	0.04	4.30	22.90	17.60	34.08	4.20	9.10	1.39	20.87	22.15
Cr₂O₃	0.00	0.01	0.00	0.04	0.00	0.01	0.00	0.00	0.00	0.03	0.02	0.08	0.00	0.00
FeO	0.15	0.00	0.18	8.00	11.00	1.19	2.30	1.99	0.32⁴⁾	15.10	17.10	11.99	22.05	23.72
MnO	0.00	0.01	0.02	0.22	0.04	0.00	0.00	0.00	0.03	0.14	0.13	0.09	5.98	1.23
MgO	23.26	32.40	31.44	20.20	25.70	23.30	32.50	25.40	0.05	13.70	11.20	11.16	0.80	1.40
CaO	15.34	0.08	0.18	12.10	0.20	13.70	0.16	0.11	25.25	11.10	10.90	22.82	11.96	13.62
K₂O	0.07	0.04	0.04	0.04	0.00	0.17	0.02	8.10	0.00	0.21	0.34	0.00	0.00	0.00
Na₂O	0.24	0.05	0.11	0.04	0.00	0.59	0.02	0.37	0.00	0.64	1.45	0.82	0.00	0.00
F	0.34	0.12	0.26	0.00	0.10	0.10	0.16	0.79	0.00	0.00	0.00	0.00	–	–
H₂O¹⁾	2.06	4.63	4.65	2.13	4.38	2.15	12.74	4.04	1.98	2.02	2.00	–	–	–
total²⁾	100.51	98.92	100.40	99.44	98.62	100.42	99.87	100.41	100.35	98.16	98.61	99.30	99.25	100.50
Cations per oxygen number	24	24	24	24	24	24	36	24	13	24	24	24	24	24
Si	7.94	7.86	7.98	7.97	7.76	7.49	5.46	5.72	2.91	7.54	6.91	7.81	6.02	5.99
Ti	0.00	0.00	0.00	0.00	0.00	0.01	0.01	0.06	0.00	0.01	0.04	0.01	0.01	0.01
Al	0.20	0.05	0.05	0.01	0.01	0.69	5.06	2.84	3.05	0.73	1.61	0.25	3.95	4.08
Cr	0.00	0.00	0.00	0.00	0.00	0.00	0.00	0.00	0.00	0.00	0.00	0.01	0.00	0.00
Fe	0.02	0.00	0.02	0.94	1.25	0.14	0.36	0.23	0.02⁴⁾	1.87	2.15	1.54	2.96	3.20
Mn	0.00	0.00	0.00	0.03	0.00	0.00	0.00	0.00	0.01	0.02	0.02	0.01	0.81	0.16
Mg	4.70	6.19	5.90	4.24	5.19	4.74	9.08	5.18	0.01	3.03	2.51	2.55	0.19	0.33
Ca	2.23	0.01	0.02	1.83	0.03	2.00	0.03	0.02	2.07	1.76	1.75	3.75	2.06	2.28
K	0.01	0.01	0.01	0.01	0.00	0.03	0.00	1.41	0.00	0.04	0.07	0.00	0.00	0.00
Na	0.06	0.01	0.03	0.01	0.00	0.16	0.01	0.10	0.00	0.18	0.42	0.25	0.00	0.00
F	0.14	0.05	0.10	0.00	0.04	0.04	0.09	0.34	0.00	0.00	0.00	0.00	–	–
OH	1.86	3.95	3.91	2.00	3.96	1.96	15.92	3.69	1.00	2.00	2.00	–	–	–
	17.06	18.13	18.02	17.04	18.24	17.26	36.02	19.59	9.05	17.18	17.48	16.16	15.99	15.95
X_{Mg}	0.996	0.999	0.996	0.814	0.806	0.972	0.962	0.985	0.746	0.616	0.537	0.623	0.048	0.091
X_{OH}	0.930	0.990	0.976	1.000	0.990	0.980	0.995	0.923	1.000	1.000	1.000	–	–	–

¹⁾ calculated based on stoichiometric (OH + F) values
²⁾ corrected for O = F
³⁾ retrograde phase
⁴⁾ Fe as Fe₂O₃
(c) = core
(r) = rim

Talc

Textures of talc show either contemporary growth of mica-like sheets with tremolite (Fig. 2) or fine grained replacement of tremolite indicating two generations of talc. These two generations cannot be distinguished chemically. Usually talc is very close to the ideal composition. Al_2O_3 is always below 0.5 wt% and there is a single sample with significant FeO contents (Gl 135, Tab. 2). It bears up to 20 mol % minnesotaite-component and coexists with actinolite (Tab. 2) and Fe-rich carbonates (Tab. 1).

Chlorite, phlogopite, zoisite

5.3 to 5.5 Si-ions per 28 oxygens classify the *chlorites* as sheridanites (HEY, 1954, Tab. 3). X_{Mg}-values of 0.96 indicate only small amounts of $FeMg_{-1}$-exchange.

Coexisting *phlogopites* have the same amounts of X_{Mg}-values (Tab. 2). As the chlorites they have some limited tschermak substitution. Significant minor element contents are TiO_2 (0.6%) Na_2O (0.4%) and CaO (0.3%). *Zoisite* is a minor constituent but when present, indicating high fugacities of H_2O since chemical composition is close to pure endmembers (Fe_2O_3 is always below 0.3%, Tab. 2) (STORRE et al., 1982).

$T-X_{CO_2}$-topology and metamorphic grade

Most marbles are chemically close to the 5-component system $CaO-MgO-SiO_2-H_2O-CO_2$. This system is very often studied experimentally but large differences in $T-X_{CO_2}$-topologies arise from different starting materials and large error brackets in connection with acute angles of intersections of reaction curves (SKIPPEN, 1971, 1974, SLAUGHTER et al., 1975, EGGERT & KERRICK, 1981, METZ & PUHAN, 1970, 1971, PUHAN & METZ, 1973). $T-X_{CO_2}$-topologies derived from natural prograde sequences of metamorphic silicates were established by TROMMSDORFF (1972) and JANSEN et al. (1978). These diagrams are only valid for the metamorphic area where they were derived from with characteristic impurities in the phases and hence are not applicable to other areas.

Fig. 9 shows the $T-X_{CO_2}$-topology which can be derived from the field investigated and is based on the following observations:

1) Disappearance of talc and calcite occurs at a slightly higher grade than the
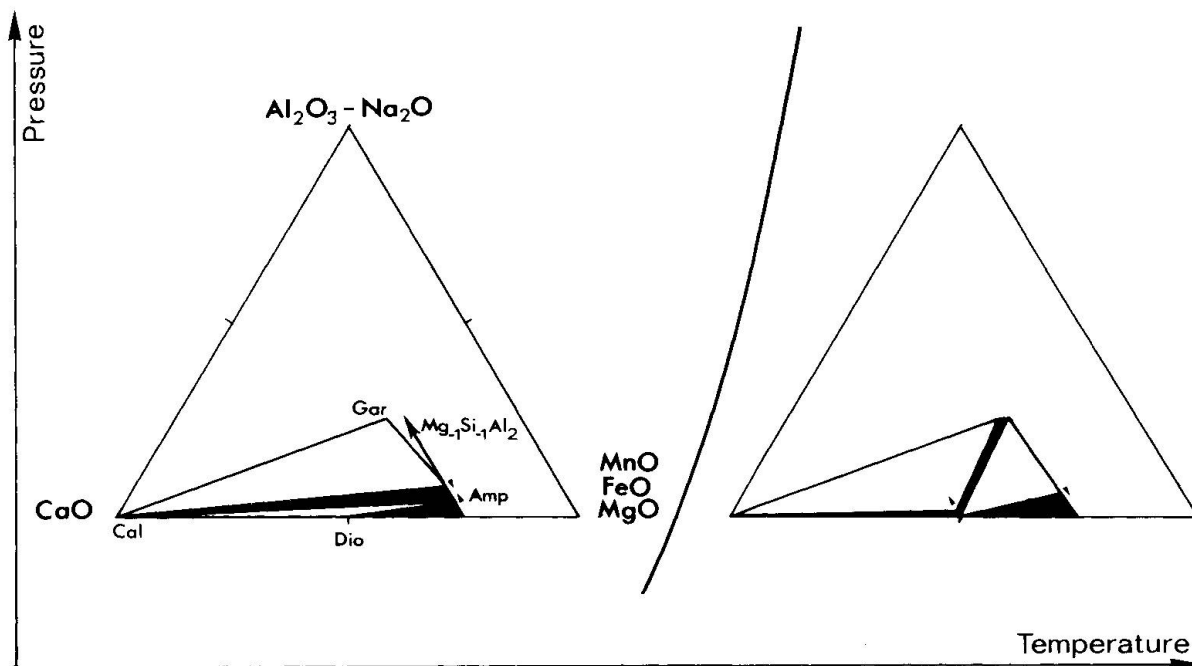
Fig. 8 Graphic representation of continuous reactions involving the tschermak vector occurring with phases of equilibrium (7). Arrows indicate presumed shift of composition of phases.
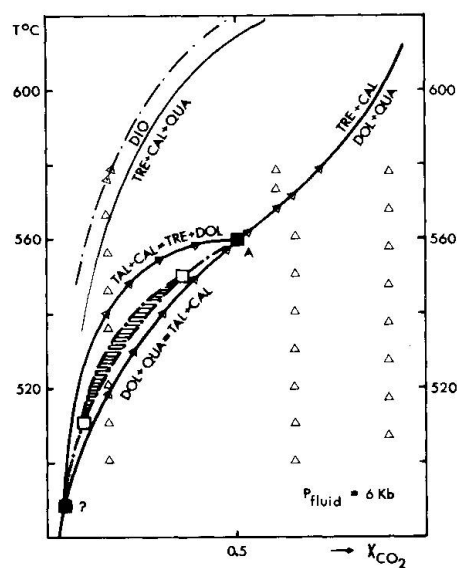

Fig. 9 T-X_{CO_2}-topology derived from the field and calcite-dolomite-geothermometry (see text.) Oblique hatched: stability field of talc and calcite in FeO-bearing metacarbonate Gl 135.
Arrows indicate path of progressive metamorphism.

first appearance of tremolite, which however is marked by significant subtitution of FeO for MgO (tab. 2, Gl 135). The temperature effects of FeO–MgO substitution on mineral equilibria are given in Tab. 3 and can be calculated from one of the available thermodynamic data sets using the equilibrium equation:

III) $\Delta G^{P,T} = \Delta H^{1,298} + {}_{298}\int^{T_\Delta} Cp\,dT - T(\Delta S^{1,298} +$

$_{298}\int^{T_\Delta} \frac{Cp}{T}\,dT) + \Delta V_s^{1,298}(P-1) + RT\ln K + RT\,\Delta\ln K$

Tab. 3 ΔK and ΔT of some equilibria due to mean values of Fe-Mg-substitution in sample GL 135.

reaction	ΔK	$\Delta \ln K$	$\Delta T°C (X_{CO_2} = 0.5)$
3 dol + 4 qua + 1 H_2O = 1 tal + 3 cal + 3 CO_2	$\left(\dfrac{0.863}{0.832}\right)^3 = 1.116$	+0.110	+ 3.5
5 dol + 8 qua + 1 H_2O = 1 tre + 3 cal + 7 CO_2	$\left(\dfrac{0.829}{0.832}\right)^5 = 0.982$	−0.018	− 0.3
5 tal + 6 cal + 4 qua = 3 tre + 2 H_2O + 6 CO_2	$\dfrac{0.829^{15}}{0.863^{15} * 0.932^6} = 0.835$	−0.180	− 2.0
2 tal + 3 cal = 1 tre + 1 dol + 1 H_2O + 1 CO_2	$\dfrac{0.829^5 * 0.832}{0.863^6} = 0.789$	−0.237	−10.8

where the equilibrium constant K equals the sum of gas-fugacities involved in the pure system and ΔK represents the change of K due to impurities in all solids involved:

(IV) $\Delta\ln K = \Sigma \ln a_s^n$

In the present case activities of tremolite, talc and dolomite were simply equaled to the mole fraction of Mg raised to the power depending on the number of sites since the only significant deviation from the pure system is due to Fe-Mg-substitution (Tab. 2) and ideal miscibility was assumed:

$a_{Mg}^{Tre} = (X_{Mg})^5$
$a_{Mg}^{Tal} = (X_{Mg})^3$
$a_{Mg}^{Dol} = X_{Mg}$

Activity of calcite coexisting with dolomite is controlled by the miscibility gap between calcite and dolomite and ΔH and ΔS in equation (III) were corrected for this effect using the equation from SKIPPEN (1974) which is based on activity coefficients from GORDON and GREENWOOD (1970):

(V) $\ln a_{CaCO_3}^{Cal} = (\dfrac{157.45}{T} - 0.253)$

For calcites not coexisting with dolomite the mole fraction X_{Ca} in calcite was taken as a_{Ca}^{Cal}.

The calculated temperature shifts to either lower (reaction 3) or higher temperatures (reaction 1) (Tab. 3) result in a reduction of the stability field of talc and calcite and the first appearance of tremolite and calcite from dolomite and quartz is lowered by about 10 °C as a result of FeO substitution.

2) Sample Gl 135 contains the assemblage (c): dol + qua + tal + cal + tre with mutual contacts between the phases (Fig. 2). This assemblage represents a unique point in an T-X_{CO_2} diagram at constant pressure and consequently allows to derive these conditions of metamorphism from experimental investigations or thermodynamic calculations. Since temperature-conditions of this assemblage are known approximately by means of the cal–dol-geothermometry in this case pressure—and X_{CO_2}—conditions may be derived from Fig. 10. In Fig. 10 the experimental and calculated data of the isobarically invariant point: dol + cal + qua + tre + tal from PUHAN & METZ (1973), SKIPPEN (1974), SLAUGHTER et al. (1975), EGGERT & KERRICK (1981) and HELGESON et al. (1978) are plotted in a P-T-diagram together with the temperature range (552 °C ± 25) due to cal–dol-thermometry. The temperature range (although only valid for the natural phases with FeO-substitution) fits rather good into the range of uncertainty of EGGERT and KERRICK (1981). Also the data from SKIPPEN (1974) are in good agreement whereas other data do not agree because they are either based on calculations with a high degree of uncertainity (SLAUGHTER et al., 1971, HELGESON et al., 1978) or on experiments with impure starting material (PUHAN and METZ, 1973, personal communication). From Fig. 10 an approximate pressure of 6 kb can be deduced which is in accordance with the appearance of kyanite in accompanying metapelites. From the discussion above it follows that the intersection point of reactions (1) to (4) in Fig. 9 was to be arranged at approximately 550 °C (6 kb) for the Fe-bearing assemblage and at 560 °C (6 kb) for the pure system.
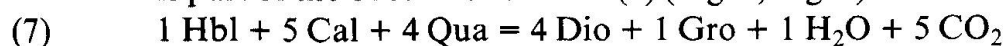
Since there is no hint for talc + calcite-stability well within the tremolite + dolomite-stability field in marbles referring to the pure system, the intersection point A cannot be situated at X_{CO_2}-values higher than 0.5.

3) The single occurrence of diopside in an impure metacarbonate sample from a region where temperature conditions of 580 °C were reached is thought to be favoured by locally low X_{CO_2}-values.

The diopside forming reaction in the pure system:

(8) $1\,Tre + 3\,Cal + 2\,Qua = 5\,Dio + 3\,CO_2 + H_2O$
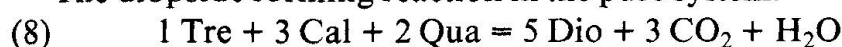
is part of the observed reaction (7) (Fig. 5, Fig. 8)

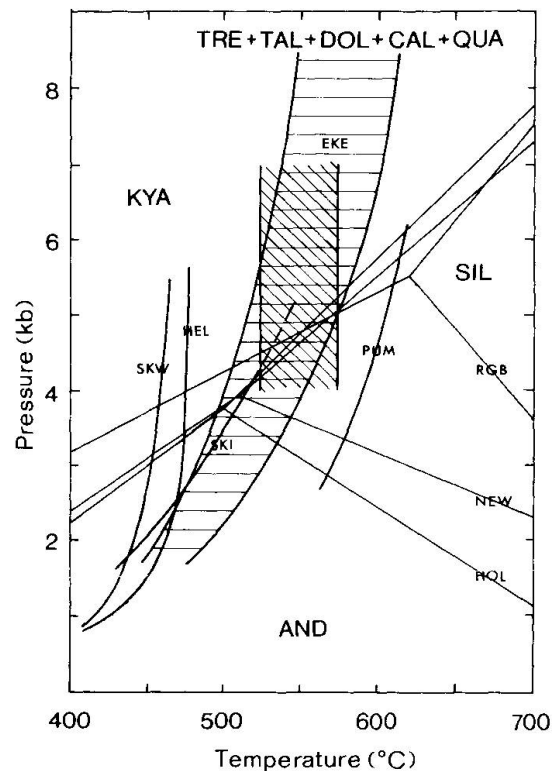(7) $1\,Hbl + 5\,Cal + 4\,Qua = 4\,Dio + 1\,Gro + 1\,H_2O + 5\,CO_2$

Fig. 10 P-T-location of the five-phase assemblage: tre + tal + dol + cal + qua according to different experimental investigations and calculation. Three locations of the kyanite–sillimanite–andalusite triple point are also shown, since kyanite occurs in neighboured metapelites. Horizontally hatched: Field of uncertainty given by EKE. Oblique hatched: Temperature according to cal-dol-thermometry.

SKW = SLAUGHTER et al. (1975), HEL = HELGESON et al. (1978), SKI = SKIPPEN (1974), EKE = EGGERT and KERRICK (1981), PUM = PUHAN and METZ (1973), RGB = RICHARDSON et al. (1969), NEW = NEWTON (1968), HOL = HOLDAWAY (1971).

Since amphiboles have higher amounts of $FeMg_{-1}$ and $Mg_{-1} Si_{-1}Al_2$ solid solution than coexisting diopside ($X_{Mg}^{Amp} = 0.54$, $X_{Mg}^{Dio} = 0.63$, $X_{Si}^{Amp} = 0.86$, $X_{Si}^{Dio} = 0.97$), equilibrium (8) is certainly shifted to higher temperatures compared with the pure system. Impurities of the solid phases are therefore not responsible for the occurrence of diopside.

The fact that rather massive dolomite + quartz marbles still occur without metamorphic reaction products must be due to different values of X_{CO_2} during metamorphism which were rather high in massive carbonate layers and rather low on fissures within massive carbonates or thin carbonate layers within metapelites.

Conclusions

Cretaceous regional metamorphism in carbonates of the Austroalpine paleozoic Schneeberg complex caused with increasing grade towards the south first

talc and tremolite followed by tremolite. Grade of metamorphism deduced from calcite–dolomite thermometry was 550 to 560°C for the assemblage Qua + Dol + Cal + Tre + Tal. This value falls well within the field of uncertainty of isobarically invariant point A given by EGGERT & KERRICK (1981) (Fig. 10). Retrograde alterations of tremolite and dolomite to talc and calcite could be demonstrated as low grade alteration (300°C) by means of calcite–dolomite thermometry.

Talc formation after tremolite therefore did not occur during but after climax conditions of Cretaceous metamorphism and tremolite must not be considered as Hercynian mineral phase.

Two reasons could be responsible for this retrograde reaction after peak of metamorphism:

1) Change in X_{CO_2} to low values and hence crossing the field of talc during cooling.

2) Change in P to low values due to uplift during peak of metamorphism which causes increase of the talc-stability field and again crossing this stability-field.during cooling.

It is not possible to argue for two episodes of metamorphism (Hercynian and Cretaceous respectively) on the basis of these textural observations. Until now only garnet textures in metapelites (HOINKES, 1981) argue for an older generation of mineral phases in this area. Cretaceous mineral ages clearly demonstrate Early Alpine amphibolite facies condition and hence present mineral assemblages are thought to be of Cretaceous age. If the Hercynian overprint in this area was relatively lower in grade compared to the Cretaceous one then enough fluid was liberated during Cretaceous dehydration and decarbonation reactions to cause the characteristic coarse grained postdeformative textures in this area.

Abbreviations:

Amp	=	Amphibole	Hbl	=	Hornblende
And	=	Andalusite	Kya	=	Kyanite
Cal	=	Calcite	Phl	=	Phlogopite
Chl	=	Chlorite	Qua	=	Quartz
Dio	=	Diopside	Sil	=	Sillimanite
Dol	=	Dolomite	Tal	=	Talc
Gar	=	Garnet	Tre	=	Tremolite
Gro	=	Grossular	Zoi	=	Zoisite

Literature

BICKLE, M.J. and R. POWELL (1977): Calcite-dolomite geothermometry for iron bearing carbonates. Contrib. Mineral. Petrol., 59, 281-292.

EGGERT, R.G. and D.M. KERRICK (1981): Metamorphic equilibria in the siliceous dolomite system: 6 kbar experimental data and geologic implications. Geochim. Cosmochim. Acta, 45, 1039-1049.

GOLDSMITH, J.R., D.L. GRAF, J. WITTERS and D.R. NORTHROP (1962): Studies in the system $CaCO_3-MgCO_3-FeCO_3$... J. Geol. 70, 659-688.

GOLDSMITH, J.R. and R.C. NEWTON (1969): P-T-X-relations in the system $CaCO_3-MgCO_3$ at high temperatures and pressures. Am. J. Sci. 267, 160-190.

GORDON, T.M. and H.J. GREENWOOD (1970): The reaction: dolomite + quartz + water = talc + calcite + carbon dioxide. Am. J. Sci. 268, 225-242.

GRAF, D.L. and J.R. GOLDSMITH (1955): Dolomite-magnesian calcite relations at elevated temperatures and CO_2 pressures. Geochim. Cosmochim. Acta, 7, 109-128.

GRAF, D.L. and J.R. GOLDSMITH (1958): The solid solubility of $MgCO_3$ in $CaCO_3$: A revision. Geochim. Cosmochim. Acta 13, 218-219.

GRAPES, R.H. and C.M. GRAHAM (1978): The actinolite-hornblende series in metabasites and the so-called miscibility gap: A review. Lithos 11, 85-97.

HARKER, R.I. and O.F. TUTTLE (1955): Studies in the system $CaO-MgO-CO_2$. Part 2: limits of solid solution along the binary join $CaCO_3-MgCO_3$. Am. J. Sci. 253, 274-282.

HELGESON, H.C., J.M. DELANY, H.W. NESBITT and D.K. BIRD (1978): Summary and critique of the thermodynamic properties of rock forming minerals. Am. J. Sci. 278-A, 1-229.

HEY, M.H. (1954): A new review of chlorites. Min. Mag. 30, 277.

HOINKES, G. und F. PURTSCHELLER (1976): Die Petrogenese der Karbonatgesteine im Schneebergzug, Ötztaler Alpen, Tirol. N. Jb. Miner. Mh. H. 10, 467-476.

HOINKES, G. (1981): Mineralreaktionen und Metamorphosebedingungen in Metapeliten des westlichen Schneebergzuges und des angrenzenden Altkristallins (Ötztaler Alpen). Tschermaks Min. Petr. Mitt. 28, 31-54.

HOLDAWAY, M.J. (1971): Stability of andalusite and the aluminum-silicate phase diagram. Am. J. Sci. 271, 97-131.

HOSCHEK, G. (1980): Phase relations of a simplified marly rock system with application to the Western Hohe Tauern (Austria). Contrib. Miner. Petrol. 73, 53-68.

JANSEN, J. B. H., A. H. VAN DE KRAATS, H. VAN DE RIJST and R. D. SCHUILING (1978): Metamorphism of siliceous dolomites at Naxos, Greece. Contrib. Miner. Petrol. 67, 279-288.

KEARNS, L. E., L. E. KITE, P. B. LEAVENS and J. A. NELEN (1980): Fluorine distribution in the hydrous silicate minerals of the Framblin marble, Orange County, New York. Am. Min. 65, 557-562.

METZ, P. and D. PUHAN (1970): Experimental investigation of the metamorphism of siliceous dolomites. I. The equilibrium data of the reaction: 3 dolomite + 4 quartz + 1 H_2O = 1 talc + 3 calcite + 3 CO_2 determined for the total pressure of 1000, 3000 and 5000 bars. Contrib. Miner. Petrol. 26, 302-314.

METZ, P. and PUHAN (1971): Korrektur zur Arbeit: Experimentelle Untersuchung zur Metamorphose von kieselig dolomitischen Sedimenten I. Contrib. Miner. Petrol. 31, 169-170.

METZ, P. (1981): Bildungsbedingungen des Diopsids in Kalksilikatparagenesen in Abhängigkeit vom Fluorgehalt des Tremolits. Fortschr. Miner. 59, Beiheft 1, 127-128.

MERCOLLI, I. (1980): Fluor-Verteilung im Tremolit und Talk in den metamorphen Dolomiten des Campolungo (Tessin) und ihre phasenpetrologische Bedeutung. Schweiz. Min. Petr. Mitt. 60, 31-44.

MOORE, J. N. and D. M. Kerrick (1976): Equilibrium in siliceous dolomites of Alta aureole, Utah. Am. J. Sci. 216, 502-524.

NESBITT, B. E. and E. J. ESSENE (1982): Metamorphic thermometry and barometry of a portion of the southern Blue Ridge province. Am. J. Sci. 282, 701-729.

NEWTON, R. C. (1968): Kyanite-andalusite equilibrium from 500 to 800°C. Science 153, 170-172.

PUHAN, D. and P. METZ (1973): in PUHAN, D. and E. HOFFER (1973): Phase relations of talc and tremolite in metamorphic calcite-dolomite sediments in the southern portion of the Damara Belt (South West Africa). Contrib. Miner. Petrol. 40, 207-214.

PUHAN, D. (1976): Metamorphic temperature determined by means of the dolomite-calcite solvus geothermometer-examples from the Central Damara Orogen (South West Africa). Contrib. Miner. Petrol. 58, 23-28.

RICE, J. M. (1977): Progressive metamorphism of impure dolomitic limestone in the Marysville aureole, Montana. Am. J. Sci. 277, 1-24.

RICHARDSON, S. W., M. C. GILBERT and P. M. BELL (1969): Experimental determination of kyanite-andalusite and andalusite-sillimanite equilibria: the aluminosilicate triple point. Am. J. Sci. 259-272.

ROSENBERG, P. E. (1967): Subsolidus relations in the system $CaCO_3-MgCO_3-FeCO_3$ between 350° and 550°C. Am. Mineral. 52, 787-796.

SATIR, M. (1975): Die Entwicklungsgeschichte der westlichen Hohen Tauern und der südlichen Ötztal-Masse auf Grund von radiometrischen Altersbestimmungen. Diss. Univ. Bern, Mem. Ist. Geol. Min. Univ. Padova, 30, 48 S.

SCHMIDEGG, O. (1933): Neue Ergebnisse in den südlichen Ötztaler Alpen. Verhandlungen Geol. B. A., Jg. 1933, 83-95.

SCHMIDT, K. E. JÄGER, M. GRÜNENFELDER und N. GRÖGLER (1967): Rb/Sr- und U/Pb-Altersbestimmungen an Proben des Ötztalkristallins und des Schneebergzuges. Eclogae Geol. Helv. 60, 529-536.

SKIPPEN, G. (1971): Experimental data for reactions in siliceous marbles. J. Geology 79, 457-481.

SKIPPEN, G. (1974): An experimental model for low pressure metamorphism of siliceous dolomitic marbles. Am. J. Sci. 274, 487-509.

SLAUGHTER, J., D. M. KERRICK and V. J. WALL (1975): Experimental and thermodynamic study of equilibria in the system $CaO-MgO-SiO_2-CO_2-H_2O$. Am. J. Sci. 275, 143-162.

STORRE, B., W. JOHANNES and K.-H. NITSCH (1982): The stability of zoisite in H_2O-CO_2 mixtures. N. Jb. Miner. Mh., Jg. 1982, H. 9, 395-406.

TALANTSEV, A. S. (1978): Revision of the dolomite-calcite geothermobarometer. Geochemistry International 15, 108-116.

THÖNI, M. (1981): Degree and evolution of the Alpine Metamorphism in the Austroalpine unit W of the Hohe Tauern in the light of K/Ar and Rb/Sr age determinations on micas. Jahrb. Geol. B.-A. 124, 111–174.

TROMMSDORFF, V. (1972): Change in T-X during metamorphism of siliceous dolomitic rocks of the Central Alps. Schweiz. Min. Petr. Mitt., 52/3, 1–4.